HHS Public Access

Author manuscript

Cell Rep. Author manuscript; available in PMC 2023 July 07.

Published in final edited form as:

Cell Rep. 2021 April 06; 35(1): 108949. doi:10.1016/j.celrep.2021.108949.

NOX1-dependent redox signaling potentiates colonic stem cell proliferation to adapt to the intestinal microbiota by linking EGFR and TLR activation

Sjoerd van der Post[1,2], **George M.H. Birchenough**[2], **Jason M. Held**[1,3,4,5,*]

[1]Department of Medicine, Washington University School of Medicine in St. Louis, St. Louis, MO, USA

[2]Department of Medical Biochemistry, Institute of Biomedicine, University of Gothenburg, Gothenburg, Sweden

[3]Department of Anesthesiology, Washington University School of Medicine in St. Louis, St. Louis, MO, USA

[4]Siteman Cancer Center, Washington University School of Medicine in St. Louis, St. Louis, MO, USA

[5]Lead contact

SUMMARY

The colon epithelium is a primary point of interaction with the microbiome and is regenerated by a few rapidly cycling colonic stem cells (CSCs). CSC self-renewal and proliferation are regulated by growth factors and the presence of bacteria. However, the molecular link connecting the diverse inputs that maintain CSC homeostasis remains largely unknown. We report that CSC proliferation is mediated by redox-dependent activation of epidermal growth factor receptor (EGFR) signaling via NADPH oxidase 1 (NOX1). NOX1 expression is CSC specific and is restricted to proliferative CSCs. In the absence of NOX1, CSCs fail to generate ROS and have a reduced proliferation rate. NOX1 expression is regulated by Toll-like receptor activation in response to the microbiota and serves to link CSC proliferation with the presence of bacterial components in the crypt. The TLR-NOX1-EGFR axis is therefore a critical redox signaling node in CSCs facilitating the quiescent-proliferation transition and responds to the microbiome to maintain colon homeostasis.

In brief

*Correspondence: jheld@wustl.edu.

AUTHOR CONTRIBUTIONS

Conceptualization, S.v.d.P. and J.M.H.; methodology, S.v.d.P., G.M.H.B., and J.M.H.; investigation, S.v.d.P. and G.M.H.B.; validation, S.v.d.P. and J.M.H.; writing – original draft, S.v.d.P. and J.M.H.; writing – review & editing, S.v.d.P. and J.M.H.

DECLARATION OF INTERESTS

The authors declare no competing interests.

SUPPLEMENTAL INFORMATION

Supplemental information can be found online at https://doi.org/10.1016/j.celrep.2021.108949.

van der Post et al. demonstrate that the ROS-generating enzyme NOX1 is highly expressed by proliferation colonic stem cells, which promote self-renewal. NOX1-dependent ROS can oxidize cysteines in EGFR to potentiate its activation and stimulate proliferation. Intestinal microbiota enhance NOX1 expression via TLR signaling to maintain colon homeostasis.

Graphical Abstract

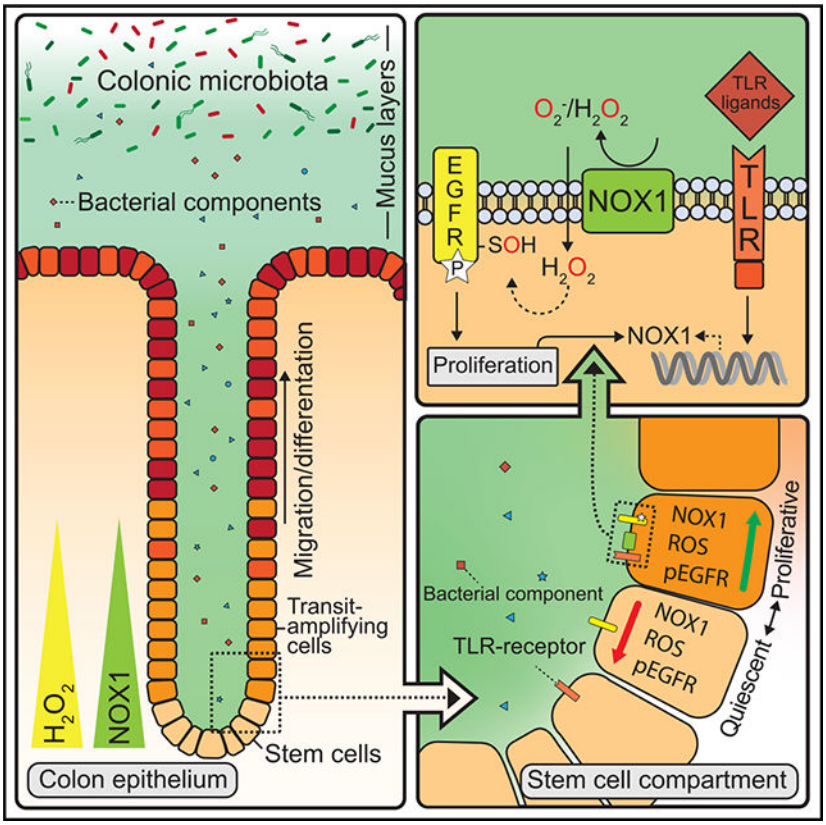

INTRODUCTION

The integrity of the intestinal epithelium is maintained by continuous cellular regeneration and depends on proliferation of stem cells at the base of each crypt in the small intestine and colon. Proliferating colonic stem cells (CSCs) transition to rapidly dividing transit-amplifying cells before terminally differentiating into one of several epithelial cell types that make up the majority of the colonic crypt (van der Flier and Clevers, 2009). However, only a small subpopulation of rapidly cycling cells is responsible for self-renewal because most CSCs are quiescent (Barker et al., 2007).

Colon homeostasis is regulated by various signals in the stem niche responsible for the transition between CSC quiescence and proliferation, as well as the CSC proliferation rate. In turn, these processes depend on cell-intrinsic factors, positioned along the crypt, as well as external cues, such as the presence of luminal microbiota (Carulli et al., 2014; Larsson et al., 2012). However, the molecular determinants integrating these diverse inputs and outputs

to tune CSC behavior and crypt maintenance are not fully understood. The WNT, NOTCH, and epidermal growth factor (EGF) receptor (EGFR) signaling pathways are essential cell-intrinsic factors responsible for maintaining CSC stemness and proliferation because chemical or genetic interference of these pathways in the crypt result in differentiation and a reduction in the size of the stem cell compartment (Barker et al., 2007; van Es et al., 2005; Wong et al., 2012). Although WNT and NOTCH are essential for CSC maintenance, EGFR signaling drives CSC proliferation, and inhibiting this pathway results in quiescence. Proliferation can be restored when EGFR inhibition is released, giving rise to the concept of a CSC "quiescent-proliferation switch" (Basak et al., 2017).

The major external stimulus of CSC proliferation is the presence of microbiota and its metabolites in the intestinal lumen. The microbiome is sensed by the colon via pattern-recognition receptors (PRRs), including Toll-like receptors (TLRs), to tune CSC proliferation. PRRs regulate the downstream transcription of genes via nuclear factor κB (NF-κB) (Takeuchi and Akira, 2010). In the absence of TLR4, or its adaptor molecule Myd88, the intestinal epithelium fails to initiate the rapid proliferation response needed to re-populate the epithelium in an induced colitis model (Santaolalla et al., 2013). Conversely, epithelial cell-specific overexpression or constitutive activation of TLR4 results in increasing numbers of proliferative cells and elongated crypts in the colon (Fukata et al., 2011). However, a mechanistic link between TLR signaling and CSC proliferation to coordinate and maintain colon homeostasis and health is not fully established (Abreu, 2010).

There are numerous reports linking redox biology with maintenance of the intestinal epithelium, primarily through the NADPH oxidase family (NOX/DUOX) (Pérez et al., 2017). DUOX2 and NOX1 are the major contributors to the generation of ROS by the colonic epithelium in the form of $O_2^{\cdot -}$ and H_2O_2 (El Hassani et al., 2005; Suh et al., 1999). Mucosal wound healing is reduced in the colon of NOX1 knockout mice because of failure of the crypts to respond by increasing proliferation, indicating that NOX1 may be an important driver of CSC proliferation (Alam et al., 2014). In addition, NOX1-dependent redox signaling enhances intestinal epithelial regeneration in response to symbiotic bacteria (Alam et al., 2014; Jones et al., 2013). NOX1 loss-of-function mutations that lack the ability to generate superoxide have been associated with very early-onset inflammatory bowel diseases, implying an important role for NOX1 in human disease pathogenesis (Hayes et al., 2015; Lipinski et al., 2019; Schwerd et al., 2018). Subunits of the NOX1 enzyme complex required for activation, such as NOXO1, have also been implicated in the regulation of proliferation in the colon (Moll et al., 2018).

However, the mechanistic details about how redox signaling directly impacts these diverse biological processes in the very dynamic intestinal epithelium are far from established. One possibility that is widely proposed is that reactive oxygen species (ROS) serve as a defensive mechanism keeping the bacteria at a distance from the colonic epithelium. This extends from the well-known role of NOX2-derived ROS in phagocytic immune cells to eliminate opsonized bacteria via generation of a high concentration of $O_2^{\cdot -}$ (Pollock et al., 1995). Defensive, cell-nonautonomous ROS is important for clearing intestinal pathogens, as shown during virulent *Salmonella* infections in mice lacking NOX2 (Cybb), which have an increased susceptibility to infection (Mastroeni et al., 2000).

However, the ROS produced by NOX in epithelial cells are generally considered to be too low a level to have a direct bactericidal effect (Botteaux et al., 2009). For example, NOX1 has been demonstrated to not substantially contribute to pathogen defense in knockout mice infected with *Salmonella typhimurium* or *Citrobacter rodentium* (Chu et al., 2016; Pircalabioru et al., 2016). Physiological levels of ROS can function in a non-defensive role by altering protein activity via oxidation of redox-sensitive cysteine thiols in proteins such as kinases and phosphates (Held, 2020; Rhee, 2006). ROS produced by NOX1 in the epithelium have been proposed to regulate colonic homeostasis by acting with both the host and in bacteria in the intestinal lumen, although the mechanistic details and signaling pathways regulated are largely unknown (Jones and Neish, 2017). Thus, the role of physiological levels of ROS produced by NOX1 in epithelial cells should be considered beneficial for maintenance of intestinal homeostasis and may act cell autonomously.

In the present study, we provide evidence that NOX1 in the colonic epithelium is specifically expressed by CSCs depending on proliferation state. Proliferating CSCs express high levels of active NOX1 compared with quiescent cells. Increased NOX1-derived ROS is responsible for redox-dependent activation of the EGFR signaling pathway, which promotes CSC proliferation. We also show that induction of NOX1 expression is regulated via the TLR-NF-κB signaling axis in response to the presence of microbiota in the colon. NOX1 is therefore an important regulator of CSC homeostasis and NOX1-dependent redox signaling mechanism connecting changes in bacterial TLR activation with EGFR activation to drive CSC proliferation. This regulatory model explains how NOX1 promotes colon epithelial turnover and maintains colon health.

RESULTS

NOX1 expression is restricted to CSCs

NOX1 has been shown to be highly expressed along the gastrointestinal tract compared with other tissues, although its celltype-specific expression within the colon remains unresolved (Suh et al., 1999). Relative mRNA expression analysis of NOX1 in mice tissue shows a gradient in expression along the entire digestive tract in a proximal-to-distal direction from stomach to colon (Figure 1A). Within the colon, NOX1 expression gradually increased through the proximal three-fourths but decreased slightly in the far distal colon.

The colonic epithelium is composed of enterocytes, goblet cells, enteroendocrine cells, and tuft cells all originating from the stem cells at the base of the crypt. To identify which cells in the colonic epithelium express NOX1, we used mouse spheroid cultures derived from the distal colon that were left undifferentiated or differentiated into absorptive or secretory cells (Basak et al., 2017; Miyoshi et al., 2017). Terminal differentiation efficiency was confirmed by probing for lineage-specific markers of stem cells (leucine-rich repeat-containing G-protein coupled receptor 5 (LGR5)), enterocytes (fatty acid-binding protein (FABP1)), and goblet cells (Mucin-2 (MUC2)) (Figure 1B). NOX1 expression was significantly reduced upon differentiation (397-fold reduction in enterocytes and 140-fold reduction in the goblet cell population, respectively), indicating that NOX1 is selectively expressed in CSCs.

To confirm the specific expression of NOX1 in colon stem cells *in vivo*, we used Lgr5-GFP knockin mice (Lgr5-EGFP-ires-CreERT2) (Barker et al., 2007). Epithelial cells were isolated 48 h after tamoxifen treatment and sorted by fluorescence-activated cell sorting (FACS) into an $EGFP^+$ stem cell or $EGFP^-$ population (Figure 1C). Analysis of the $EGFP^+$ and $EGFP^-$ population for NOX1 expression, along with the stem cell markers achaetescute homolog 2 (ASCL2) and LGR5, were found to be highly enriched in the $EGFP^+$ cell populations, confirming that NOX1 expression is restricted to CSCs. Lgr5-EGFP-IRES-creERT2 expression is known to be variegated in the intestinal epithelium, resulting in some $EGFP^-$ stem cells after recombination. Thus, the high degree of enrichment of LGR5, ASCL2, and NOX1 in $EGFP^+$ cells indicates the very specific expression of NOX1 in CSCs *in vivo*.

In addition, NOX1 localization was confirmed to be at the base of the colonic crypt and absent in the underlying tissue using *in situ* hybridization (Figure 1D). A negative control for the NOX1 *in situ* hybridization probe in $NOX1^{y/-}$ tissue had no signal, confirming the probe specificity (Figure S1A). *In situ* hybridization was also performed on distal ileum tissue to confirm the observed low NOX1 expression level in the small intestine (Figure 1A). Only low NOX1 expression was observed, which was spatially restricted to the base of the crypt (Figure S1B). NOX1 expression is therefore restricted to $LGR5^+$ CSCs at the base of the crypt and highly abundant in the colon.

NOX1 is the major source of ROS in CSCs

NOX1 and DUOX2, another NOX family member, are the major producers of ROS in the intestinal epithelium (Lambeth, 2004; Pircalabioru et al., 2016). To determine which NOX family member was the major contributor to ROS production in CSCs, we first assessed their relative expression. DUOX2 mRNA expression in stem cell-enriched colonic spheroid cultures was found to be three orders of magnitude lower than NOX1 (Figure S2A). Upon differentiation, DUOX2 expression was increased in both the enterocyte and goblet cell populations (Figure S2B). The limited expression of DUOX2 in CSCs is consistent with previous findings in which DUOX2 was found to be expressed primarily at the tip of the crypts (Sommer and Bäckhed, 2015). The spatial separation of NOX1 and DUOX2, as well as the cell-type-specific expression, indicates they have distinct roles in the colonic epithelium.

The role of NOX1 as the exclusive ROS-generating enzyme in CSCs was further established with the use of spheroid cultures derived from wild-type and $NOX1^{y/-}$ mice. The catalytic activity of NOX1 was measured with the luminescent probe L-012 ($O_2^{\cdot -}$) or Amplex red (H_2O_2). The generation of both forms of ROS was significantly reduced in the $NOX1^{y/-}$ colonic spheroids and could be inhibited to baseline by the NOX1 inhibitor ML171 in wild-type spheroids (Figures 2A and 2B). Notably, these assays were performed in the absence of phorbol-12 myristate 13-acetate (PMA) that stimulates NOX enzyme activity, indicating that NOX1 in CSCs has high intrinsic basal activity. NOX activity independent of stimulation was previously observed in guinea pig primary intestinal cultures and is in contrast with colon cancer lines where NOX1 activation requires PMA (Kawahara et al.,

2004). These results indicate that high levels of active NOX1 are found in CSCs at the base of the crypt, where it is the predominant source of basal ROS generation.

NOX1-derived ROS promote CSC proliferation

ROS have been implicated to be an important transducer of proliferative signaling in several epithelial model systems (Dickinson et al., 2011; Ranjan et al., 2006). To establish if NOX1$^{y/-}$ deletion affected CSC proliferation, we performed time-course imaging comparing NOX1$^{y/-}$ with wild-type spheroid cultures. NOX1$^{y/-}$ spheroids showed a significant reduction in growth with no effect on spheroid formation, indicating that the growth deficit is due to a decreased proliferative rate (Figure 3A; Video S1). Treatment of the spheroid cultures with *N*-acetyl cysteine (NAC), a general antioxidant, reduced the growth of both wild-type and NOX1$^{y/-}$ spheroids significantly (Figures 3B and 3C). NOX1-derived ROS are therefore required to maintain basal proliferation in CSCs.

We next quantified the role of NOX1 on CSC proliferation *in vivo* in both the distal and proximal colon by short-term 5-ethynyl-2′-deoxyuridine (EdU) incorporation. We observed a significant reduction in the number of cells in S-phase compared with NOX1 mutant animals in the distal colon, while no changes were observed in the proximal colon, which expresses less NOX1 (Figures 3D and 3E). These results show that NOX1 is needed for stem cell proliferation in both primary spheroid cultures and *in vitro* in the distal region of the colon, where it is predominantly expressed.

NOX1 expression and activity in CSCs are a marker for proliferation state

The majority of the CSCs at the crypt base are found in a quiescent state, and only a small subset of fast cycling proliferative cells are responsible for the renewal of the epithelium. The switch between these two states can be mediated by the growth factors WNT and EGF, as well as environmental factors, such as the bacterial-derived short-chain fatty acid butyrate, an histone deacetylase (HDAC) inhibitor that is found in high concentrations in the colonic lumen (Kaiko et al., 2016; Sato et al., 2011). The EGFR signaling pathway is essential to maintain CSCs in a proliferative state, because inhibition or withdrawal of EGFR ligands leads to CSC quiescence that can be reactivated to reinstate proliferation (Basak et al., 2017). To address if NOX1 was differentially expressed in proliferative versus quiescent CSCs, we treated spheroids with gefitinib to block EGFR activity and proliferation. We observed a significant reduction in spheroid growth upon EGFR inhibition in conditioned media, confirming that the cells become quiescent (Figure 4A). mRNA expression of NOX1 was significantly reduced in spheroids induced into quiescence by either inhibition of EGFR or upon treatment with butyrate (Figure 4B). Upon removal of butyrate, CSCs re-enter the cell cycle and continue to proliferate as indicated by the reinstated expression of marker of proliferation Ki67 (MKi67) and cyclin B1 (CCNB1) coinciding with NOX1 expression (Figure 4C). NOX1 expression is therefore tightly regulated by the proliferation state in CSCs.

Next, we addressed if altered NOX1 mRNA expression in quiescent versus proliferating spheroids would parallel its enzymatic activity and ROS production. NOX1-derived $O_2^{\cdot -}$ production was measured with luminol in quiescent spheroid cultures treated with either

gefitinib or butyrate. Both inhibitors resulted in reduced enzyme activity, comparable with the level observed in NOX1$^{y/-}$ cultures (Figure 4D).

We next assessed if NOX1 was expressed in proliferating cells in the distal colon *in vivo* by co-localizing NOX1 expression by *in situ* hybridization with short-term EdU treatment to mark proliferating cells. The colocalization of NOX1 to EdU was similar to the *in situ* hybridization pattern of the canonical proliferation marker MKi67 (Figure 4E). NOX1 expression was restricted to the stem cell compartment, and an average of 83% of the cells in S-phase were NOX1-expressing, comparable with the MKi67 expression profile (Figure 4F). These results indicate that actively cycling CSCs *in vitro* and *in vivo* express high levels of NOX1 and generate ROS, which is distinct from quiescent CSCs.

NOX1-derived ROS regulate proliferation by potentiating EGFR activity

The data implicating NOX1-dependent redox signaling in CSC proliferation led to the question of which proliferation-dependent signaling pathways were activated by NOX1 activity. Because EGFR activation is essential for CSC proliferation, we determined whether NOX1 is involved in its activation. In addition, EGFR activity has been shown to be regulated via H_2O_2 by direct sulfenylation of a cysteine in its kinase domain independent of ligand binding (Heppner et al., 2016; Truong et al., 2016).

EGFR phosphorylation was reduced in the NOX1$^{y/-}$ spheroids cultured under serum-free conditions, indicating that NOX1 activity potentiates EGFR activation in the absence of its ligand. In addition, the antioxidant NAC reduced EGFR activity in wild-type, but not NOX1$^{y/-}$, spheroids, confirming the redox and NOX1 dependence of EGFR phosphorylation in CSCs (Figure 5A). To determine if EGFR is redox modified in a NOX1-dependent manner, we assayed its cysteine sulfenation by treating spheroid cultures *ex vivo* with DYn-2 (Yang et al., 2015). Sulfonated EGFR was detected only in wild-type cells, indicating that EGFR activation is redox regulated by NOX1 in CSCs (Figure 5B).

To further delineate the role of NOX1 in EGFR signaling, we supplemented spheroid cultures with EGF for 48 h. This restored the proliferation defect observed in NOX1$^{y/-}$ spheroids to the level of the control spheroid cultures (Figure 5C). We confirmed this result by evaluating if the addition of EGF resulted in an increased number of proliferative cells in S-phase by EdU incorporation. In wild-type cultures, the average percentage of proliferative cells was 22.2% (±3) independent of EGF treatment, while in NOX1$^{y/-}$ spheroids, the percentage increased significantly from an average of 8.0% to 20.4% upon EGF treatment (Figure 5D). Because NOX1$^{y/-}$ spheroids can respond to EGF, this suggests that NOX1 functions in parallel or upstream to EGFR. However, because EGFR inhibition itself also affects NOX1 levels (Figure 4), placing NOX1 downstream of EGFR, we propose that NOX1 and EGFR are regulated by a feedback loop that is described in the Discussion.

Growth factor stimulation of receptor tyrosine kinases has been shown to result in a transient increase in intracellular ROS (Bae et al., 1997; Rhee, 2006). To confirm that EGF treatment of CSCs increased intracellular ROS levels via NOX1, we quantified ROS production in EGF-stimulated spheroids. Treatment with EGF increased intracellular ROS levels in

a NOX1-dependent manner, and an overall higher basal level of intracellular ROS was observed in the wild-type cells compared with NOX1 mutants (Figures 5E and 5F).

Taken together, increased NOX1 activity and ROS formation in proliferating CSCs redox-modifies and potentiates EGFR signaling to support basal proliferation.

Microbial components induce TLR-dependent NOX1 expression and proliferation in CSCs

Because NOX1 was observed to directly affect EGFR signaling, we next focused on how NOX1 expression was regulated. In addition to basal proliferation, colonic epithelial turnover is regulated by the presence of microbial components, so we focused on the impact of the microbiome on NOX1 expression and function (Thursby and Juge, 2017). NOX1 has been shown to be regulated and activated in intestinal epithelial cells in response to microbial components via PRRs, including TLRs, but to date this has not been functionally linked to the stem cell compartment (Kawahara et al., 2004; Ogier-Denis et al., 2008).

We observed that spheroid cultures established from the different regions between the proximal and distal colon upon passaging (Figure 6A) did not maintain the differential NOX1 expression observed *in vivo* (Figure 1A). This suggested that an external stimulus was absent in our *ex vivo* spheroid culture model system. Because the *in vivo* NOX1 expression gradient coincides with the increase in bacterial load toward the distal colon, we hypothesized that NOX1 expression might be regulated in response to microbial components (Donaldson et al., 2016). Spheroids derived from the distal colon were stimulated with three different microbial-derived TLR ligands: flagellin, lipopolysaccharide (LPS), or lipoteichoic acid. NOX1 expression was significantly increased in response to all three TLR ligands (Figure 6B). Next, we confirmed if TLR ligands affected proliferation in a NOX1-dependent manner by treating spheroids for up to 72 h with varying LPS concentrations. Wild-type spheroids grew significantly larger over time, while in $NOX1^{y/-}$, reduced growth was observed (Figures 6C and 6D). This indicates that NOX1 acts downstream of the TLR pathway to mediate CSC proliferation. The unexpected reduction in growth in $NOX1^{y/-}$ spheroids upon chronic LPS treatment is potentially due to pleiotropic effects of TLR signaling that are independent of NOX1.

TLR receptors signal by activating the NF-κB pathway primarily via Myd88. To determine if NOX1 is a downstream target of NF-κB and induced by TLR signaling, we quantified NOX1 mRNA expression upon inhibition of the interleukin-1 receptor-associated kinase 4 (IRAK4), which is an essential effector of the NF-κB pathway. This was performed in combination with LPS to stimulate TLR signaling. NOX1 transactivation was inhibited upon IRAK4 inhibition, confirming that NOX1 is downstream of NF-κB in CSCs (Figure 6E). Expression analysis of additional known NF-κB targets confirmed the efficiency of IRAK4 inhibition (Figure S3).

In contrast, basal NOX1 expression was independent of NF-κB signaling. Spheroid cultures derived from $Myd88^{-/-}$ mice had a similar level of NOX1 mRNA expression compared with wild type. No significant increase in NOX1 mRNA expression was observed in $Myd88^{-/-}$ spheroids upon LPS treatment (Figure 6F), similar to IRAK4 inhibition, confirming the TLR dependence of NOX1 induction. To determine if the regulation of NOX1-derived ROS

production required NF-κB activation, we determined spheroid $O_2^{\cdot -}$ generation capacity by luminol in wild-type, Myd88$^{-/-}$, and NOX1$^{y/-}$ spheroids in the presence or absence of different TLR ligands. No significant difference in NOX1 activity was observed between Myd88$^{-/-}$ and wild-type spheroids in the absence of TLR stimulation, while upon LPS stimulation a significant increase in ROS was observed between wild-type and Myd88$^{-/-}$ (Figure 6G). Together, these indicate that NOX1 is preferentially regulated via Myd88.

The increase in ROS production by LPS stimulation in Myd88$^{-/-}$ cells implied that TLR4 may act in part via TRIF-dependent signaling. We further evaluated this by stimulating spheroids with the TLR3 ligand polyinosinic-polycytidylic acid (poly(I:C)), which acts exclusively via TRIF, which did not induce a ROS response. None of the TLR ligands induced increased $O_2^{\cdot -}$ generation in the NOX1$^{y/-}$, confirming NOX1 dependence (Figure 6G). The functional effect of the lack of an inducible NOX1 response on CSC proliferation was evaluated in Myd88$^{-/-}$ spheroids. In contrast with wild-type spheroids, Myd88$^{-/-}$ spheroids did not increase proliferation upon LPS stimulation (Figure 6H).

Taken together, induction of NOX1 mRNA and ROS production by TLR signaling mediated by Myd88 and NF-κB increases CSC proliferation.

Microbial depletion and colonization affect NOX1 expression and cell proliferation *in vivo*

To validate the bacterial dependence of NOX1 regulation *in vivo*, we treated mice with a combination of broad-specific antibiotics to reduce the colonic microbial load (Figure S4A). The mRNA expression level of NOX1 was significantly reduced in the distal colon when less bacteria were present, whereas no effect was observed in the proximal colon (Figure 6I). Next, we determined the number of proliferative cells (EdU$^+$) by flow cytometry after antibiotic treatment in the two colon regions, comparing wild-type and NOX1$^{y/-}$ mice. In the distal colon, the number of proliferative cells in the NOX1$^{y/-}$ mice at baseline was reduced significantly as observed earlier based on histology. Antibiotics further reduced the number of proliferating cells, but there was no longer a proliferation difference between wild-type and NOX1$^{y/-}$ mice (Figure 6J). These results indicate that NOX1 expression is regulated by the presence of microbiota *in vivo*, where it increases CSC proliferation in the distal colon. Conversely, NOX1 expression is not affected by antibiotic treatment in the proximal colon (Figure 6I), which coincides with no NOX1-dependent change in CSC proliferation by changes in microbiota content (Figure 6J).

The induction of NOX1 expression by microbiota *in vivo* was further characterized by conventionalizing (Conv-D) germ-free (GF) mice using microbiota from conventionally raised (ConvR) mice. Microbial colonization is established and maintained at Conv-R level after 1 week of conventionalization (Figure S4B). Introduction of bacteria to the intestine of GF mice induced a significant proliferative response that was maintained over a 4-week time period (Figures 6K and 6M) and coincided with a significant increase in NOX1 expression (Figure 6L). At week 4, the increase in NOX1 expression and crypt length diminished and were comparable with GF and Conv-R mice, indicating that homeostasis had been largely restored. Basal NOX1 expression level at steady state in GF, Conv-R, and Myd88$^{-/-}$ mice was also at a comparable level, as expected (Figure 6L). In contrast, NOX1 expression was not significantly increased in the proximal colon at any time point during

conventionalization (Figure S4C). In addition, the fluorescent *in situ* hybridization signal for NOX1 was stronger and present in more cells at the crypt base in the distal colon upon conventionalization (Figure 6N).

These data describe a mechanism by which the commensal microbiota regulate epithelial turnover via TLR-dependent induction of NOX1 expression in CSCs that can be adapted in response to increased or reduced microbial content.

DISCUSSION

The molecular determinants of CSC homeostasis are poorly understood, especially how CSCs sense external changes in the microbiome and stimulate subsequent proliferation to maintain the integrity of the intestinal epithelium. In addition, although the functional benefit of NOX1-generated H_2O_2 in maintaining homeostasis, self-renewal, and differentiation is established (Pérez et al., 2017), the molecular mechanisms by which redox signaling underlies these diverse biological processes are far from understood. Our study reports a role for redox regulation in the colon by directly linking the expression of NOX1 to proliferating stem cells at the base of the crypt compartment, where its activity enhances proliferation via redox activation of EGFR signaling in a feedback loop upon bacterial sensing (Figure 7). The marked switch in NOX1 expression between proliferating and quiescent CSCs is induced via changes in intestinal bacterial load via the TLR-NF-κB signaling pathway. Thus, NOX1-derived ROS serve as a sensor mechanistically linking changes in the microbiota to CSC proliferation, which maintains colon homeostasis.

We find that NOX1 is a bona fide marker of proliferating stem cells, similar to MKi67. Under basal conditions, only a small subset of proliferative cells are responsible for continuous self-renewal of the epithelium, while the majority of the CSCs are in a quiescent state acting as a clonogenic reserve (Barker et al., 2007). We show that NOX1 expression and ROS production are tightly regulated during the transition into a proliferative state in concordance with, and to the same extent as, canonical cell-cycle genes such as Cyclin-B1. The coregulation of NOX1 and cell-cycle genes is highly specific to stem cells in the colon (Kaiko et al., 2016). The transient and short window of proliferation means that NOX1-derived ROS can be produced briefly at high levels to potentiate the quiescent-proliferation transition and proliferation rate before being downregulated upon differentiation to minimize oxidative stress.

The molecular mechanism of NOX1 in CSC proliferation and the quiescent-proliferation switch is via redox activation of the EGFR pathway. NOX1-derived ROS directly redox-modify and modulate EGFR activity in our colonic CSC model system in which wild-type spheroids were capable of maintaining EGFR activation in the absence of the EGF ligand for an extended time period compared with $NOX1^{y/-}$ mutants (Jagadeesha et al., 2012). The addition of antioxidants reduced CSC proliferative capacity and EGFR phosphorylation, indicating the redox dependency of EGFR activation. Antioxidants or NOX inhibitor treatment results in reduced intracellular H_2O_2 generation and signal transduction upon growth factor stimulation (ten Freyhaus et al., 2006; Sundaresan et al., 1995). We observed a substantial increase in NOX1-dependent intracellular ROS upon EGF stimulation in CSCs,

indicating that a similar signal transduction mechanism responsible for potentiating EGFR-driven proliferation is present in the intestine. These results are consistent with the fact that physiological levels of H_2O_2 can activate EGFR independent of ligand binding via the redox modification of a key regulatory cysteine within the EGFR kinase domain (Heppner et al., 2016; Truong and Carroll, 2012). To date, the mechanistic importance of ROS in CSC proliferation has been only established in the context of colorectal cancer, where the GTPase RAC1 activates NOX1 upon APC loss to drive hyperproliferation (Cheung et al., 2016; Myant et al., 2013). Rescuing the NOX1-dependent proliferation phenotype via treatment with exogenous H_2O_2, which is rapidly metabolized and targets different cysteines than endogenously produced H_2O_2 (Behring et al., 2020; Millonig et al., 2012), is not technically feasible. However, our results are consistent with the other studies demonstrating that H_2O_2 is the key mediator of NOX1-dependent proliferation (Arnold et al., 2001).

The cell-autonomous role of NOX1-derived ROS may also have a non-mutually exclusive antimicrobial role whereby ROS also prevents bacterial invasion into crypt. Antimicrobial activity has been clearly demonstrated for DUOX2, which, in contrast with NOX1, is solely expressed at the tip of the crypt in closer proximity to the luminal microbiota (Sommer and Bäckhed, 2015). The role of NOX1-dependent ROS as both a mediator of CSC self-renewal and bacterial defense acting in parallel could be at the base of an improved wound repair in mouse (Kato et al., 2016; Leoni et al., 2013).

In the intestine, host-microbe interactions signal via TLRs, which are required to maintain intestinal homeostasis and are essential for epithelial renewal during wound healing (Rakoff-Nahoum et al., 2004). NOX1 expression and activity in the intestine have been implicated in the response to the abundant microbiota in the intestinal lumen, but its role and regulation remain unresolved (Aviello and Knaus, 2018; Jones and Neish, 2017). We find that there are two roles of NOX1 activity in CSCs. First, basal NOX1 expression and activity potentiate CSC proliferation at steady state. Second, an adaptive response by stimulation with bacterial components can further augment NOX1 activity in a TLR-Myd88-dependent manner. The role of NOX1 in epithelial homeostasis in the colon at steady state is supported by similar basal NOX1 expression in wild-type, GF, and $Myd88^{-/-}$ mice. In addition, basal proliferation of CSCs *in vivo* and *ex vivo* is decreased in the absence of NOX1.

Complementarily to this intrinsic role of NOX1 in CSCs, we show that NOX1 expression can also be induced via TLR signaling in order to adapt to changes in the microbiome. We observed that both proliferation and NOX1 expression were significantly reduced specifically in the distal colon of mice upon antibiotic treatment. The observed reduction in proliferation after antibiotics treatment in the NOX1 mutant indicates that the microbiota can affect proliferation in the colon through NOX1-independent routes. In addition, GF mice colonized with intestinal microbiota provoked an increase in both proliferation and NOX1 expression over a 4-week time window, but after this period both returned to baseline. This indicates there is an adaptive NOX1 response upon bacterial exposure. Given the functional role of NOX1 in the colon, the inducible NOX1 response serves to protect the host when needed. The importance of TLR-inducible NOX1 expression is also essential during epithelial wounding or in dextran sulfate-induced colitis models, where NOX1 plays

an important functional role in reconstituting the damaged epithelium in NOX1 knockout mice (Kato et al., 2016; Leoni et al., 2013).

CSCs grown *ex vivo* lose the distinct proximal-to-distal NOX1 expression gradient observed *in vivo*, indicating the importance of host-microbiome interactions on NOX1 expression. Furthermore, microbial stimulation with ligands for TLR2, TLR4, and TLR5 induced NOX1 expression in spheroid cultures, providing a direct mechanistic link between the microbiota and NOX1-dependent CSC proliferation. This TLR-dependent response is consistent with an increase in bacterial density along the gut axis that correlates with NOX1 expression. These findings highlight the host's potential to adapt CSC proliferation in response to bacterial presence via TLR signaling.

The presence of niche signals such as WNT and EGF are essential for intestinal crypt maintenance and provided by interspersed supporting epithelial and mesenchymal cells (Gehart and Clevers, 2019). Although Paneth cells are absent in the colon, they play a similar supportive role as NOX1 at the crypt base in the small intestine by secreting growth factors that promote stem cell proliferation and self-renewal in addition to their role in anti-microbial defense. It is possible that NOX1-generated ROS have a similar function in the distal colon by compensating for the reduced growth factor levels in the absence of Paneth cells.

NOX1 plays a critical role in colonic crypt homeostasis, acting as a key driver of redox signaling responsible for CSC proliferation and maintenance of the epithelial barrier in response to the microbiota. Our findings demonstrate that NOX1 is a specific marker for proliferative stem cells in the colonic crypt capable of potentiating proliferation by inducible ROS generation. NOX1-derived ROS act cell intrinsically in proliferating CSCs to potentiate EGFR signaling. This signaling axis can be directly induced by bacterial components, establishing a mechanistic link between the TLR and EGFR pathways that dynamically increases CSC proliferation in response to changes in the microbiota that enables restoration of homeostasis. Our findings also provide a plausible, cell-autonomous explanation for the development of very early onset of inflammatory bowel disease in patients with NOX1 mutations whereby imbalanced CSC adaptation in response to the microbiota ultimately triggers a prolonged immune response.

STAR★METHODS

RESOURCE AVAILABILITY

Lead contact—Further information and requests for resources and reagents should be directed to and will be fulfilled by the Lead Contact, Jason M. Held (jheld@wustl.edu).

Materials availability—This study did not generate new unique reagents.

Data and code availability—This study did not generate any unique datasets or code.

EXPERIMENTAL MODEL AND SUBJECT DETAILS

Animals—The NOX1$^{-/-}$, Lgr5-EGFP-IRES-creERT2, and C57BL/6 mice were obtained from Jackson Laboratories (Bar Harbor, ME, USA) and all experiments were approved by the Washington University in St Louis institutional animal care and use committee. Myd88$^{-/-}$ and germ-free mice experiments were performed at the University of Gothenburg according to Gothenburg laboratory animal ethics committee guidelines. Mice were housed in a specific pathogen free facility with access to chow and water *ad libitum*. Animals were used for experiments in the age range between 8 and 12 weeks, and all were littermate control males. Males were selected as the NOX1 gene is X-linked only allowing male littermate breeding.

Primary cell culture—Mouse spheroid cultures were established and cultured as described previously (Miyoshi and Stappenbeck, 2013). Briefly crypts were isolated from either the proximal or distal colon of eight week old male mice after collagenase digestion (Millipore) for 45 minutes. After removal of the intestinal tissue crypts were pelleted by centrifugation and embedded in Matrigel (Corning) in 24 or 48-well plates. The cultures were passaged three times before used for experiments. Stem cell media was composed of 50% conditioned media in DMEM/F12 (GIBCO) supplemented with GlutaMAX (GIBCO), 100U Penicillin-Streptomycin (GIBCO), 10μM Y27632 (Cayman) with a final FBS concentration of 10%. Conditioned media was prepared from L-WRN cells (gift from T. Stappenbeck, ATCC, CRL-3276) engineered to secrete Wnt3a, R-spondin and noggin, filtered and frozen until use.

METHOD DETAILS

Mice treatments—Mice received a combination of vancomycin, neomycin, ampicillin and metronidazole (Sigma) with the addition of 1% glucose for one-week *ad libitum*. Proliferation was assessed 2 hr after inter peritoneum injection with 5-Ethynyl-2′-deoxyuridine (Cayman). Cre recombineering in the Lgr5-EGFP-IRES-creERT2 mice was achieved after a single inter peritoneum injection with 200 μL tamoxifen (10mg/mL) (Sigma). Conventionalized (Conv-D) mice were generated by colonizing germ-free (GF) C57BL/6 mice with caecal/faecal microbiota from conventionally raised (Conv-R) C57BL/6 donors. For each experiment, caecal and colonic content was harvested from three ConvR donors under aseptic conditions. Caecal/faecal content was pooled in 10 mL PBS supplemented with 0.1% (w/v) cysteine (Sigma) and homogenized using a T10 ULTRA-TURRAX rotor stator homogenizer (IKA). Freshly prepared homogenate (200 μl) was immediately administered to GF mice via gavage, and the resulting Conv-D mice were subsequently housed under conventional conditions for the duration of the experiment. Female donor and recipient mice were used for all conventionalization experiments.

Primary intestinal epithelial cell treatment—For differentiation assays spheroids were trypsinized with TrypLE Express (GIBCO) for 1 minute, re-embedded into matrigel (Corning) and cultured for 24 hr in DMEM/F12, 10μM Y27632, 5 ng/mL EGF with either 5 μM DAPT for goblet cell cultures or 10 μM L-161,982 for enterocyte cultures. Spheroid growth was assessed over 48 to 72 hour time windows obtaining four bright field images at 10x per well at 1 hr. intervals using a Incucyte ZOOM (Essen BioSciences) microscope,

or for full well endpoint stitched images were obtained for long-term treatment with LPS (Sigma), EGF (R&D systems) or n-acetyl cysteine (Sigma) using a BioTek Cytation5 automated microscope. Data analysis was performed in Fiji for 100 spheroids per condition and represented as sphere surface in mm^2.

mRNA isolation and real-time quantitative PCR—Spheroids were treated for 4 hr before RNA extraction with 1μM ultrapure lipopolysaccharide (InvivoGen), 1 μM lipoteichoic acid (Sigma) or 0.1 μM flagellin (Sigma) with or without pretreatment with 10 μM PF06650833 (Sigma). Quiescence conditions were induced by 18 or 36 hr treatment with 1 mM butyrate (Sigma) or 5 μM Gefitinib (Cayman). Snap frozen tissue or spheroids in matrigel were recovered and homogenized in RLT buffer (QIAGEN). Tissue samples were homogenized with the use of an Ultra Turbax homogenizer T10 (IKA). RNA was extracted using the RNAeasy micro kit (QIAGEN) and converted to cDNA using random hexamers (High-capacity cDNA kit, Applied biosystems). qPCR analysis were performed using PowerUp SYBR green (Applied Biosystems) and analyzed on a CFX96 (Bio-Rad) thermocycler and relative abundance changes were calculated using the delta-delta-ct method by normalization to GAPDH and ACTB expression.

Gel electrophoresis and immunoblot analysis—Spheroids were cultured under serum free conditions in DMEM/F12 with or without 1mM n-acetylcysteine (NAC) for 6 hr and recovered from matrigel using Cell Recovery Solution (Corning) with the addition of phosphatase inhibitor cocktail 2, 3 and 10mM sodium fluoride (Sigma-Aldrich). Matrigel droplets were incubated for 30 minutes on an end-over-end mixer at 4°C, followed by centrifugation at 750 × g for 5 minutes. Pelleted spheres were washed once with PBS, lysed in RIPA buffer and the protein concentration was determined by BCA (Invitrogen). Lysates were resolved by electrophoresis on 4%–12% gradient NuPAGE Bis-Tris gels (Invitrogen). Proteins were transferred to nitro cellulose by electroblotting (TransBlot Turbo, BioRad). Blots were blocked with 5% BSA in TBST and probed with the following primary antibodies for 1 hr anti EGFR (2232, Cell Signaling) or phosphoylated EGFR Tyr-1068 (3777, Cell Signaling) and detected with HRP conjugated goat anti-rabbit antibody. Blots were imaged by chemiluminescence after treatment with ECL substrate (BioRad).

Flow cytometry analysis and cell sorting—For FACS analysis epithelial cells from Lgr5-EGFP-IRES-creERT2 mice were isolated from the last 3 cm of the distal colon 48 hr after tamoxifen treatment. Tissue was opened longitudinal washed three time in PBS then cut into smaller pieces and transferred to cold HBBS (Ca^{2+} and Mg^{2+} free) with 5 mM EDTA and incubated for 75 min on an end-over-end mixer at 4°C. Crypts were pelleted by centrifugation after vigorously shaking and removal of the tissue. Single cell suspensions were achieved by digestion with TrypLE (GIBCO) for 30 min in HBBS with 10mg/mL DNase (Roche) at 37°C. The isolated cells from three mice were pooled and sorted into two populations (EGFP+ and EGFP−) by FACS (Sony SY3200) collected in RLT lysis buffer (QIAGEN) and directly processed for mRNA extraction as described earlier. To quantify cells in S-phase spheroid cultures were incubated for 2 hr with 10 μM 5-Ethynyl-2′-deoxyuridine (EdU) after which cells were recovered from the matrigel with 5 mM EDTA and digested into single cells using TrypLE for 45 minutes at 37°C. Cells

were fixed in 4% PFA for 15 minutes washed in with 2% BSA in PBS and sulfo-Cy5 azide (Lumiprobe) was conjugated using click-it chemistry. For the click reaction cell pellets were incubated for 30 minutes in 50 μL 2 μM azidesulfo-Cy5, 2 mM CuSO4, 100 mM ascorbic acid in PBS followed by two 15 min. washes in 2% BSA in PBS. The above procedure was also followed to determine *in vivo* EdU incorporation, isolating single cell using EDTA and TrypLE as described. Flow cytometry analysis were performed on a FACScan instrument (Becton Dickinson) and data were analyzed using FlowJo v10 (FlowJo LLC). Intracellular ROS was assayed after incubation for 2 hr with 5 μM CellROX green (Molecular probes). Single cell suspensions were generated as described above with the addition of 2 mM NAC during the TrypLE digestion. Cells were kept on ice in the dark and directly analyzed as described.

Detection of sulfenylated proteins—To label sulfenylated protein cysteines spheroid cultures were incubated with 2 mM DYn2 [4-(pent-4-yn-1-yl)cyclohexane-1,3-dione] (Cayman) for 1 hr. Spheroids were recovered and cell lysis was performed as described above in the presence of 5 mM NAC. Labeled proteins were biotinylated via click-chemistry with 100μM Biotin-Picolyl-Azide (Click Chemistry Tools) in a reaction with the following components 500μM THPTA [tris-hydroxypropyltriazolylmethylamine] (Click Chemistry Tools), 100μM $CuSO_4$ and 5mM ascorbate, incubated for 30 min. Excess reagents were removed by filtration using molecular weight cutoff filters (Pall). Biotin labeled protein were enriched using prewashed streptavidin agarose in spin columns (Pierce) for 1 hr end-over-end mixing, washed twice for 30 minutes with 0.5% SDS followed by centrifugation. Eluted proteins were resolved by electrophoresis, transferred to nitro cellulose and EGFR was detected by as described earlier.

Hydrogen peroxide and superoxide detection—Superoxide detection was performed using L-012 in spheroid cultures in the presence of 2.5 μg/mL LPS, 2.5 μg/mL Poly(I:C) HMW (Invivogen), 20 μM ML171 (Tocris), 1 mM butyrate (Sigma) or 5 μM Gefitinib (Cayman). Cells in matrigel were recovered in prewarmed 37°C Krebb-ringer bicarbonate buffer containing 100 μM L-012 (FUJIFILM, Wako) and transferred to white 96-well plate. Luminescence was measured over a 30 minutes time window at 37°C using an Infinite m200 (Tecan) or CLARIOstar (BMG Labtech) plate reader. Spheroids were isolated from the matrigel using recovery solution as described before and BCA was used to quantify the protein concentration used to normalize the assay results. H_2O_2 generation was measured using the Amplex red assay (Thermo Fisher). 100μL of 0.2U/mL HRP, 20μM Amplex red in preheated 37°C Krebs-ringer bicarbonate buffer was added to each condition and incubated for 1 hr. at 37°C. The reaction was quenched and spheroids were disrupted by adding 20 μL 5 mM EDTA and the supernatant was transferred to a 96 well plate. In parallel a standard H_2O_2 curve was made prepared to determine the absolute nmol concentration in the samples. Analyzes were performed on using an Infinite m200 plate reader (Tecan) at excitation 530 nm and emission 600 nm.

Imaging—NOX1 *in situ* hybridization combined with antibody staining and EdU detection was performed on distal colon tissue collected from mice 2 hr after receiving an intraperitoneal injection with 100 μL 20 mM EdU. Dissected tissue was fixed for 16

hr in 4% formaldehyde, paraffin embedded, dewaxed, pretreatment, antigen retrieval and single molecule *in situ* hybridization of NOX1 (probe: 464651) or Mki67 (416771) was performed according to manufacturer's instructions RNAscope fluorescent reagent kit v2 (ACD, Bio-Techne) visualized with Opal-570 (Perkin-Elmer). Detection of EdU positive cells was achieved by incubating the sections for 30 minutes with 4 μM azide-picolyl-A488 (Jena Bioscience), 2 mM $CuSO_4$, 100 mM ascorbic acid in PBS followed by two 15 minutes washed in PBS. For immunohistochemistry sections were blocked with 1%BSA in PBS and incubated overnight with rabbit Epcam (1:200, Abcam, ab71916) followed by the secondary Alexa647 goat anti-rabbit antibody (Invitrogen). Nuclei were counterstained with Hoechst 33528 (1μg/ml) and images were obtained by confocal microscope (Zeiss LSM 700). Imaging of S-phase cells in wild-type and $NOX1^{y/-}$ mice was done on proximal and distal colon tissue fixed in 4% PFA for 1 hr and embedded in OCT (Fisher) for cryosectioning. EdU incorporation was detected by click conjugation of azide-sulfo-Cy5 (Lumiprobe) as above and images were obtained by fluorescent microscopy (Olympus IX70). Images were analyzed in Imaris (Bitplane) or Fiji and statistical analysis were performed in Prism v8 (Graphpad).

QUANTIFICATION AND STATISTICAL ANALYSIS

Statistical analysis was performed using Prism v7 (GraphPad). All data is presented as mean ± standard error or the mean (SEM). Unpaired two-tailed t tests or one-way ANOVA with Tukey's post test for correction of multiple comparisons was performed between groups. A cut off at $p < 0.05$ was used for statistical significance. Details regarding the statistical test used in the respective experiments are indicated in the figure legends together with populations size.

Supplementary Material

Refer to Web version on PubMed Central for supplementary material.

ACKNOWLEDGMENTS

We would like to thank Fredrik Backed and Louise Mannerås Holm for providing the GF mice. We acknowledge funding and support from the National Institutes of Health (NIH) grant R01CA200893 (J.H.), (The Swedish Research Council (Vetenskapsrådet [V]) grant 2015-00656 (S.v.d.P.), Swedish Society for Medical Research (Svenska Sällskapet för Medicinsk Forskning) grant P17-0060 (S.v.d.P.), NIH grant 5U01AI095545-08 (G.M.H.B.), and VR grant 2018–02278 (G.M.H.B.).

REFERENCES

Abreu MT (2010). Toll-like receptor signalling in the intestinal epithelium: how bacterial recognition shapes intestinal function. Nat. Rev. Immunol. 10, 131–144. [PubMed: 20098461]

Adachi O, Kawai T, Takeda K, Matsumoto M, Tsutsui H, Sakagami M, Nakanishi K, and Akira S (1998). Targeted disruption of the MyD88 gene results in loss of IL-1- and IL-18-mediated function. Immunity 9, 143–150. [PubMed: 9697844]

Alam A, Leoni G, Wentworth CC, Kwal JM, Wu H, Ardita CS, Swanson PA, Lambeth JD, Jones RM, Nusrat A, and Neish AS (2014). Redox signaling regulates commensal-mediated mucosal homeostasis and restitution and requires formyl peptide receptor 1. Mucosal Immunol. 7, 645–655. [PubMed: 24192910]

Arnold RS, Shi J, Murad E, Whalen AM, Sun CQ, Polavarapu R, Parthasarathy S, Petros JA, and Lambeth JD (2001). Hydrogen peroxide mediates the cell growth and transformation caused by the mitogenic oxidase Nox1. Proc. Natl. Acad. Sci. USA 98, 5550–5555. [PubMed: 11331784]

Aviello G, and Knaus UG (2018). NADPH oxidases and ROS signaling in the gastrointestinal tract. Mucosal Immunol. 11, 1011–1023. [PubMed: 29743611]

Bae YS, Kang SW, Seo MS, Baines IC, Tekle E, Chock PB, and Rhee SG (1997). Epidermal growth factor (EGF)-induced generation of hydrogen peroxide. Role in EGF receptor-mediated tyrosine phosphorylation. J. Biol. Chem. 272, 217–221. [PubMed: 8995250]

Barker N, van Es JH, Kuipers J, Kujala P, van den Born M, Cozijnsen M, Haegebarth A, Korving J, Begthel H, Peters PJ, and Clevers H (2007). Identification of stem cells in small intestine and colon by marker gene Lgr5. Nature 449, 1003–1007. [PubMed: 17934449]

Basak O, Beumer J, Wiebrands K, Seno H, van Oudenaarden A, and Clevers H (2017). Induced Quiescence of Lgr5+ Stem Cells in Intestinal Organoids Enables Differentiation of Hormone-Producing Enteroendocrine Cells. Cell Stem Cell 20, 177–190.e4. [PubMed: 27939219]

Behring JB, van der Post S, Mooradian AD, Egan MJ, Zimmerman MI, Clements JL, Bowman GR, and Held JM (2020). Spatial and temporal alterations in protein structure by EGF regulate cryptic cysteine oxidation. Sci. Signal. 13, eaay7315. [PubMed: 31964804]

Botteaux A, Hoste C, Dumont JE, Van Sande J, and Allaoui A (2009). Potential role of Noxes in the protection of mucosae: H(2)O(2) as a bacterial repellent. Microbes Infect. 11, 537–544. [PubMed: 19298864]

Carulli AJ, Samuelson LC, and Schnell S (2014). Unraveling intestinal stem cell behavior with models of crypt dynamics. Integr. Biol. 6, 243–257.

Cheung EC, Lee P, Ceteci F, Nixon C, Blyth K, Sansom OJ, and Vousden KH (2016). Opposing effects of TIGAR- and RAC1-derived ROS on Wnt-driven proliferation in the mouse intestine. Genes Dev. 30, 52–63. [PubMed: 26679840]

Chu F-F, Esworthy RS, Doroshow JH, and Shen B (2016). NADPH oxidase-1 deficiency offers little protection in *Salmonella typhimurium*-induced typhlitis in mice. World J. Gastroenterol. 22, 10158–10165. [PubMed: 28028364]

Dickinson BC, Peltier J, Stone D, Schaffer DV, and Chang CJ (2011). Nox2 redox signaling maintains essential cell populations in the brain. Nat. Chem. Biol. 7, 106–112. [PubMed: 21186346]

Donaldson GP, Lee SM, and Mazmanian SK (2016). Gut biogeography of the bacterial microbiota. Nat. Rev. Microbiol. 14, 20–32. [PubMed: 26499895]

El Hassani RA, Benfares N, Caillou B, Talbot M, Sabourin J-C, Belotte V, Morand S, Gnidehou S, Agnandji D, Ohayon R, et al. (2005). Dual oxidase2 is expressed all along the digestive tract. Am. J. Physiol. Gastrointest. Liver Physiol. 288, G933–G942. [PubMed: 15591162]

Fukata M, Shang L, Santaolalla R, Sotolongo J, Pastorini C, España C, Ungaro R, Harpaz N, Cooper HS, Elson G, et al. (2011). Constitutive activation of epithelial TLR4 augments inflammatory responses to mucosal injury and drives colitis-associated tumorigenesis. Inflamm. Bowel Dis. 17, 1464–1473. [PubMed: 21674704]

Gehart H, and Clevers H (2019). Tales from the crypt: new insights into intestinal stem cells. Nat. Rev. Gastroenterol. Hepatol. 16, 19–34. [PubMed: 30429586]

Hayes P, Dhillon S, O'Neill K, Thoeni C, Hui KY, Elkadri A, Guo CH, Kovacic L, Aviello G, Alvarez LA, et al. (2015). Defects in NADPH Oxidase Genes NOX1 and DUOX2 in Very Early Onset Inflammatory Bowel Disease. Cell. Mol. Gastroenterol. Hepatol. 1, 489–502. [PubMed: 26301257]

Held JM (2020). Redox Systems Biology: Harnessing the Sentinels of the Cysteine Redoxome. Antioxid. Redox Signal. 32, 659–676. [PubMed: 31368359]

Heppner DE, Hristova M, Dustin CM, Danyal K, Habibovic A, and van der Vliet A (2016). The NADPH Oxidases DUOX1 and NOX2 Play Distinct Roles in Redox Regulation of Epidermal Growth Factor Receptor Signaling. J. Biol. Chem. 291, 23282–23293. [PubMed: 27650496]

Jagadeesha DK, Takapoo M, Bánfi B, Bhalla RC, and Miller FJ Jr. (2012). Nox1 transactivation of epidermal growth factor receptor promotes N-cadherin shedding and smooth muscle cell migration. Cardiovasc. Res. 93, 406–413. [PubMed: 22102727]

Jones RM, and Neish AS (2017). Redox signaling mediated by the gut microbiota. Free Radic. Biol. Med. 105, 41–47. [PubMed: 27989756]

Jones RM, Luo L, Ardita CS, Richardson AN, Kwon YM, Mercante JW, Alam A, Gates CL, Wu H, Swanson PA, et al. (2013). Symbiotic lactobacilli stimulate gut epithelial proliferation via Nox-mediated generation of reactive oxygen species. EMBO J. 32, 3017–3028. [PubMed: 24141879]

Kaiko GE, Ryu SH, Koues OI, Collins PL, Solnica-Krezel L, Pearce EJ, Pearce EL, Oltz EM, and Stappenbeck TS (2016). The Colonic Crypt Protects Stem Cells from Microbiota-Derived Metabolites. Cell 165, 1708–1720. [PubMed: 27264604]

Kato M, Marumo M, Nakayama J, Matsumoto M, Yabe-Nishimura C, and Kamata T (2016). The ROS-generating oxidase Nox1 is required for epithelial restitution following colitis. Exp. Anim. 65, 197–205. [PubMed: 26876598]

Kawahara T, Kuwano Y, Teshima-Kondo S, Takeya R, Sumimoto H, Kishi K, Tsunawaki S, Hirayama T, and Rokutan K (2004). Role of nicotinamide adenine dinucleotide phosphate oxidase 1 in oxidative burst response to Toll-like receptor 5 signaling in large intestinal epithelial cells. J. Immunol. 172, 3051–3058. [PubMed: 14978110]

Knoop KA, Gustafsson JK, McDonald KG, Kulkarni DH, Coughlin PE, McCrate S, Kim D, Hsieh C-S, Hogan SP, Elson CO, et al. (2017). Microbial antigen encounter during a preweaning interval is critical for tolerance to gut bacteria. Sci. Immunol. 2, eaao1314. [PubMed: 29246946]

Lambeth JD (2004). NOX enzymes and the biology of reactive oxygen. Nat. Rev. Immunol. 4, 181–189. [PubMed: 15039755]

Larsson E, Tremaroli V, Lee YS, Koren O, Nookaew I, Fricker A, Nielsen J, Ley RE, and Bäckhed F (2012). Analysis of gut microbial regulation of host gene expression along the length of the gut and regulation of gut microbial ecology through MyD88. Gut 61, 1124–1131. [PubMed: 22115825]

Leoni G, Alam A, Neumann P-A, Lambeth JD, Cheng G, McCoy J, Hilgarth RS, Kundu K, Murthy N, Kusters D, et al. (2013). Annexin A1, formyl peptide receptor, and NOX1 orchestrate epithelial repair. J. Clin. Invest. 123, 443–454. [PubMed: 23241962]

Lipinski S, Petersen B-S, Barann M, Piecyk A, Tran F, Mayr G, Jentzsch M, Aden K, Stengel ST, Klostermeier UC, et al. (2019). Missense variants in NOX1 and p22phox in a case of very-early-onset inflammatory bowel disease are functionally linked to NOD2. Cold Spring Harb. Mol. Case Stud. 5, a002428. [PubMed: 30709874]

Mastroeni P, Vazquez-Torres A, Fang FC, Xu Y, Khan S, Hormaeche CE, and Dougan G (2000). Antimicrobial actions of the NADPH phagocyte oxidase and inducible nitric oxide synthase in experimental salmonellosis. II. Effects on microbial proliferation and host survival in vivo. J. Exp. Med. 192, 237–248. [PubMed: 10899910]

Millonig G, Ganzleben I, Peccerella T, Casanovas G, Brodziak-Jarosz L, Breitkopf-Heinlein K, Dick TP, Seitz H-K, Muckenthaler MU, and Mueller S (2012). Sustained submicromolar H2O2 levels induce hepcidin via signal transducer and activator of transcription 3 (STAT3). J. Biol. Chem. 287, 37472–37482. [PubMed: 22932892]

Miyoshi H, and Stappenbeck TS (2013). In vitro expansion and genetic modification of gastrointestinal stem cells in spheroid culture. Nat. Protoc. 8, 2471–2482. [PubMed: 24232249]

Miyoshi H, VanDussen KL, Malvin NP, Ryu SH, Wang Y, Sonnek NM, Lai CW, and Stappenbeck TS (2017). Prostaglandin E2 promotes intestinal repair through an adaptive cellular response of the epithelium. EMBO J. 36, 5–24. [PubMed: 27797821]

Moll F, Walter M, Rezende F, Helfinger V, Vasconez E, De Oliveira T, Greten FR, Olesch C, Weigert A, Radeke HH, and Schröder K (2018). NoxO1 Controls Proliferation of Colon Epithelial Cells. Front. Immunol. 9, 973. [PubMed: 29867954]

Myant KB, Cammareri P, McGhee EJ, Ridgway RA, Huels DJ, Cordero JB, Schwitalla S, Kalna G, Ogg E-L, Athineos D, et al. (2013). ROS production and NF-κB activation triggered by RAC1 facilitate WNT-driven intestinal stem cell proliferation and colorectal cancer initiation. Cell Stem Cell 12, 761–773. [PubMed: 23665120]

Ogier-Denis E, Mkaddem SB, and Vandewalle A (2008). NOX enzymes and Toll-like receptor signaling. Semin. Immunopathol. 30, 291–300. [PubMed: 18493762]

Pérez S, Taléns-Visconti R, Rius-Pérez S, Finamor I, and Sastre J (2017). Redox signaling in the gastrointestinal tract. Free Radic. Biol. Med. 104, 75–103. [PubMed: 28062361]

Pircalabioru G, Aviello G, Kubica M, Zhdanov A, Paclet M-H, Brennan L, Hertzberger R, Papkovsky D, Bourke B, and Knaus UG (2016). Defensive Mutualism Rescues NADPH Oxidase Inactivation in Gut Infection. Cell Host Microbe 19, 651–663. [PubMed: 27173933]

Pollock JD, Williams DA, Gifford MA, Li LL, Du X, Fisherman J, Orkin SH, Doerschuk CM, and Dinauer MC (1995). Mouse model of X-linked chronic granulomatous disease, an inherited defect in phagocyte superoxide production. Nat. Genet. 9, 202–209. [PubMed: 7719350]

Rakoff-Nahoum S, Paglino J, Eslami-Varzaneh F, Edberg S, and Medzhitov R (2004). Recognition of commensal microflora by toll-like receptors is required for intestinal homeostasis. Cell 118, 229–241. [PubMed: 15260992]

Ranjan P, Anathy V, Burch PM, Weirather K, Lambeth JD, and Heintz NH (2006). Redox-dependent expression of cyclin D1 and cell proliferation by Nox1 in mouse lung epithelial cells. Antioxid. Redox Signal. 8, 1447–1459. [PubMed: 16987002]

Rhee SG (2006). Cell signaling. H2O2, a necessary evil for cell signaling. Science 312, 1882–1883. [PubMed: 16809515]

Santaolalla R, Sussman DA, Ruiz JR, Davies JM, Pastorini C, España CL, Sotolongo J, Burlingame O, Bejarano PA, Philip S, et al. (2013). TLR4 activates the b-catenin pathway to cause intestinal neoplasia. PLoS ONE 8, e63298–e15. [PubMed: 23691015]

Sato T, van Es JH, Snippert HJ, Stange DE, Vries RG, van den Born M, Barker N, Shroyer NF, van de Wetering M, and Clevers H (2011). Paneth cells constitute the niche for Lgr5 stem cells in intestinal crypts. Nature 469, 415–418. [PubMed: 21113151]

Schwerd T, Bryant RV, Pandey S, Capitani M, Meran L, Cazier J-B, Jung J, Mondal K, Parkes M, Mathew CG, et al. ; WGS500 Consortium; Oxford IBD cohort study investigators; COLORS in IBD group investigators; UK IBD Genetics Consortium; INTERVAL Study (2018). NOX1 loss-of-function genetic variants in patients with inflammatory bowel disease. Mucosal Immunol. 11, 562–574. [PubMed: 29091079]

Sommer F, and Bäckhed F (2015). The gut microbiota engages different signaling pathways to induce Duox2 expression in the ileum and colon epithelium. Mucosal Immunol. 8, 372–379. [PubMed: 25160818]

Suh YA, Arnold RS, Lassegue B, Shi J, Xu X, Sorescu D, Chung AB, Griendling KK, and Lambeth JD (1999). Cell transformation by the superoxide-generating oxidase Mox1. Nature 401, 79–82. [PubMed: 10485709]

Sundaresan M, Yu Z-X, Ferrans VJ, Irani K, and Finkel T (1995). Requirement for generation of H2O2 for platelet-derived growth factor signal transduction. Science 270, 296–299. [PubMed: 7569979]

Takeuchi O, and Akira S (2010). Pattern recognition receptors and inflammation. Cell 140, 805–820. [PubMed: 20303872]

ten Freyhaus H, Huntgeburth M, Wingler K, Schnitker J, Bäumer AT, Vantler M, Bekhite MM, Wartenberg M, Sauer H, and Rosenkranz S (2006). Novel Nox inhibitor VAS2870 attenuates PDGF-dependent smooth muscle cell chemotaxis, but not proliferation. Cardiovasc. Res. 71, 331–341. [PubMed: 16545786]

Thursby E, and Juge N (2017). Introduction to the human gut microbiota. Biochem. J. 474, 1823–1836. [PubMed: 28512250]

Truong TH, and Carroll KS (2012). Redox regulation of epidermal growth factor receptor signaling through cysteine oxidation. Biochemistry 51, 9954–9965. [PubMed: 23186290]

Truong TH, Ung PM-U, Palde PB, Paulsen CE, Schlessinger A, and Carroll KS (2016). Molecular Basis for Redox Activation of Epidermal Growth Factor Receptor Kinase. Cell Chem. Biol. 23, 837–848. [PubMed: 27427230]

van der Flier LG, and Clevers H (2009). Stem cells, self-renewal, and differentiation in the intestinal epithelium. Annu. Rev. Physiol. 71, 241–260. [PubMed: 18808327]

van Es JH, van Gijn ME, Riccio O, van den Born M, Vooijs M, Begthel H, Cozijnsen M, Robine S, Winton DJ, Radtke F, and Clevers H (2005). Notch/g-secretase inhibition turns proliferative cells in intestinal crypts and adenomas into goblet cells. Nature 435, 959–963. [PubMed: 15959515]

Wong VWY, Stange DE, Page ME, Buczacki S, Wabik A, Itami S, van de Wetering M, Poulsom R, Wright NA, Trotter MWB, et al. (2012). Lrig1 controls intestinal stem-cell homeostasis by negative regulation of ErbB signalling. Nat. Cell Biol. 14, 401–408. [PubMed: 22388892]

Yang J, Gupta V, Tallman KA, Porter NA, Carroll KS, and Liebler DC (2015). Global, in situ, site-specific analysis of protein S-sulfenylation. Nat. Protoc. 10, 1022–1037. [PubMed: 26086405]

Highlights

- NOX1 expression is restricted to proliferating stem cells in the colonic epithelium
- NOX1-EGFR-TLR is a redox signaling node critical to maintaining colon homeostasis
- Expression of NOX1 is regulated in response to the microbiota via TLR signaling

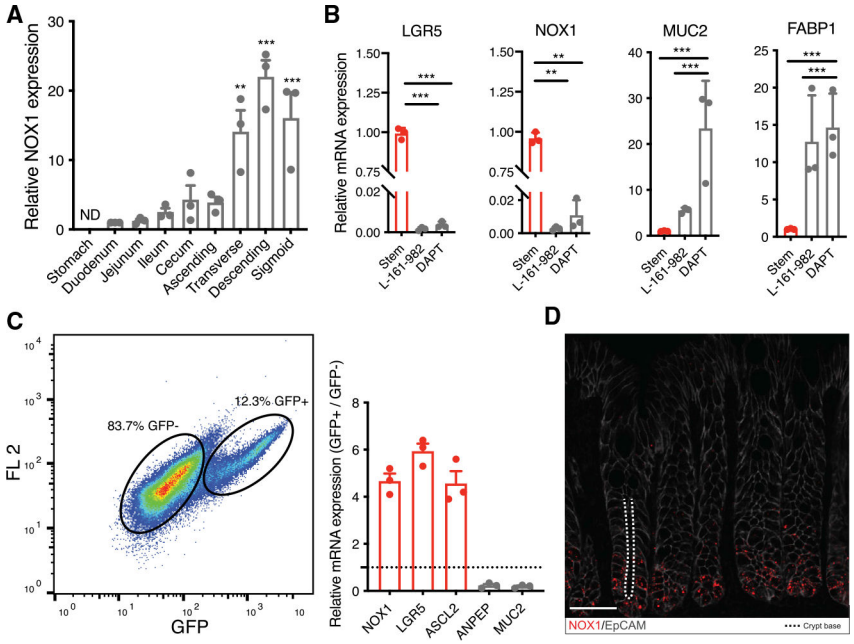

Figure 1. NOX1 expression increases along the length of the intestine, and its expression is restricted to stem cells

(A) Expression of NOX1 along the gastrointestinal tract of mice assessed by qPCR. Data are presented as fold change compared with duodenum (n = 3). Data are represented as mean ± SEM.

(B) Relative mRNA expression of LGR5, NOX1, MUC2, and FABP1 in undifferentiated spheroids (stem cells) or differentiated into enterocytes (L-161–982) or goblet cells (DAPT) (n = 3). Data are represented as mean ± SD.

(C) FACS isolation of LGR5-EGFP^{+} and LGR5-EGFP^{-} distal colon epithelial cells and the relative mRNA expression of cell-type markers in the two sorted populations. Data are represented as mean ± SEM.

(D) *In situ* hybridization of NOX1 in distal colon tissue. Scale bars, 30 μm. **p < 0.01, ***p < 0.001 by one-way ANOVA and Tukey's posttest.

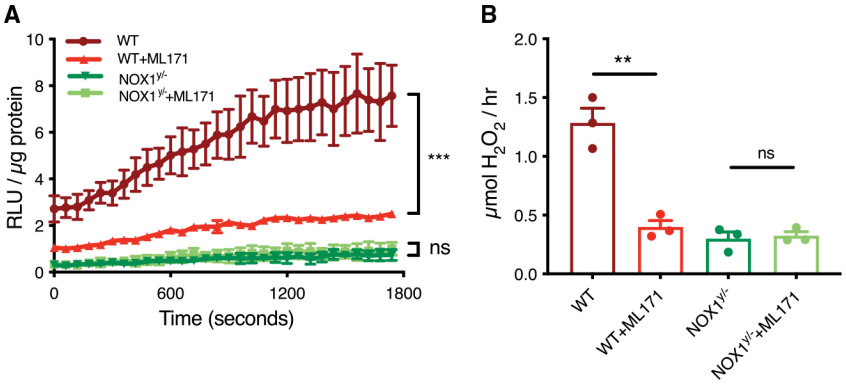

Figure 2. NOX1 is the major source of H_2O_2 and $O_2 \cdot -$ in colonic stem cells

(A) $O_2 \cdot -$ production over 30 min in wild-type (WT) and NOX1$^{y/-}$ spheroid cultures treated with the NOX1 inhibitor ML171 quantified with L-012 (n = 3). ***p < 0.001 by two-way ANOVA with Sidak's correction for multiple comparison.

(B) H_2O_2 production per hour by WT and NOX1$^{y/-}$ stem cultures treated with the NOX1 inhibitor ML171 quantified with the H_2O_2-specific probe Amplex red (n = 3). **p < 0.01 by one-way ANOVA and Tukey's posttest. Data are represented as mean ± SEM.

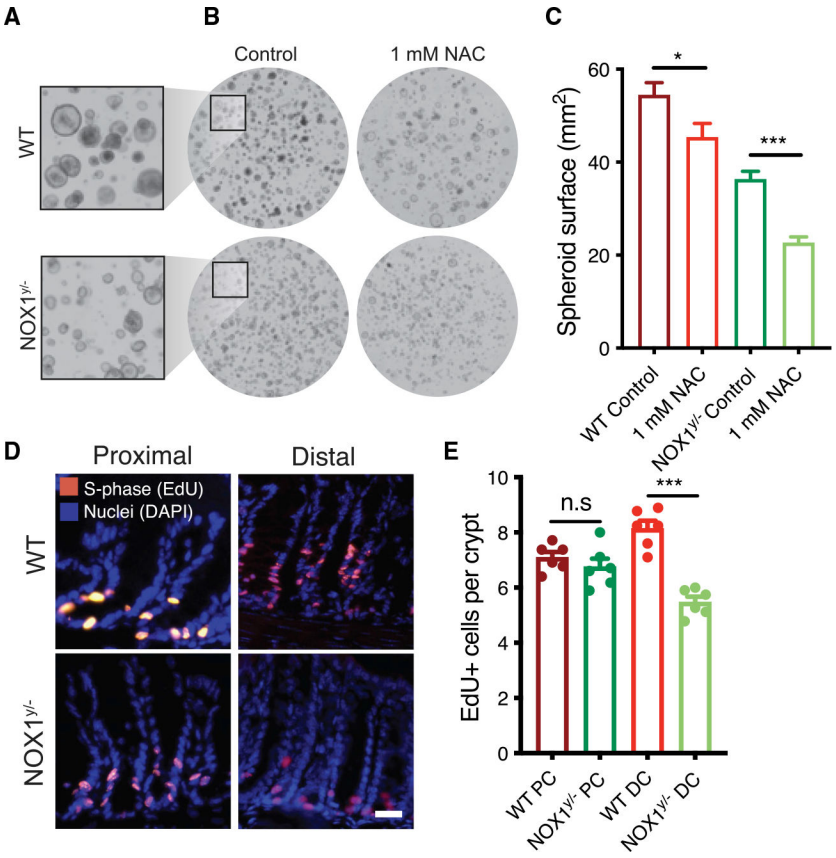

Figure 3. NOX1 affects colonic stem cell proliferation

(A) Representative images of WT and NOX1$^{y/-}$ spheroid cultures.

(B and C) Spheroid growth of WT and NOX1$^{y/-}$ cultures treated for 48 h with media containing 1 mM NAC (B) and measurements of spheroid growth (n = 3, 100 spheroids) (C).

(D) Representative images of proliferative cells (EdU^{+}) in crypts of WT and NOX1$^{y/-}$ distal and proximal colon from mice treated with EdU for 2 h.

(E) Quantification of the number of EdU^{+} cells per crypt in the proximal (PC) and distal colon (DC) of WT and NOX1$^{y/-}$ mice (n = 6, 7–12 crypts).

Scale bars, 25 μm. *p < 0.05, ***p < 0.001 by one-way ANOVA and Tukey's posttest. Data are represented as mean ± SEM.

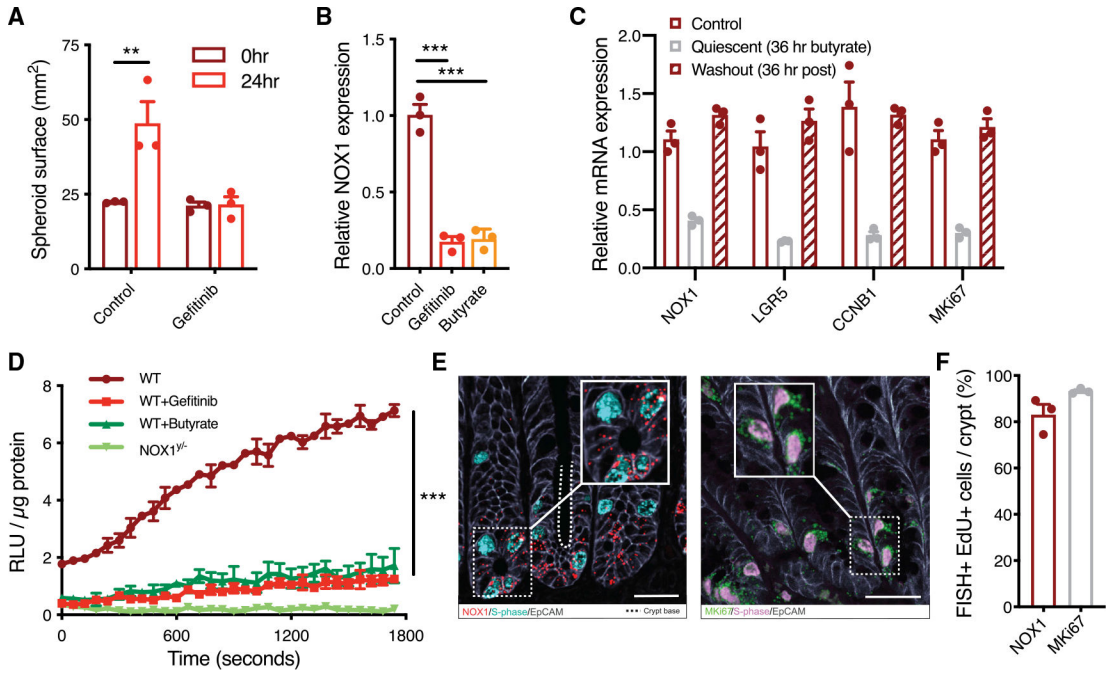

Figure 4. NOX1 activity and expression are restricted to CSCs during proliferation

(A) Surface of WT spheroids before and after treatment for 24 h with the EGFR inhibitor gefitinib (n = 3, 100 spheroids).

(B) qPCR analysis of NOX1 expression in WT spheroid cultures treated for 24 h with the EGFR inhibitor gefitinib or the HDAC inhibitor butyrate (n = 3).

(C) Relative mRNA expression analysis for LGR5, NOX1, CCNB1, and MKi67 in control, butyrate-induced quiescence, and washout spheroids (n = 3).

(D) Superoxide generation in WT and $NOX1^{y/-}$ cultures treated for 24 h with 1 mM gefitinib or 5 µM butyrate over 30 min (n = 3).

(E) Detection of S-phase cells and NOX1 or MKi67 mRNA expression by *in situ* hybridization in mouse distal colon sections.

(F) Percentage of cells in both S-phase (EdU^+) and NOX1 or MKi67 positive (n = 3, 15 crypts).

**p < 0.01, ***p < 0.001 by one-way ANOVA and Tukey's posttest. Data are represented as mean ± SEM. Scale bars, 30 µm.

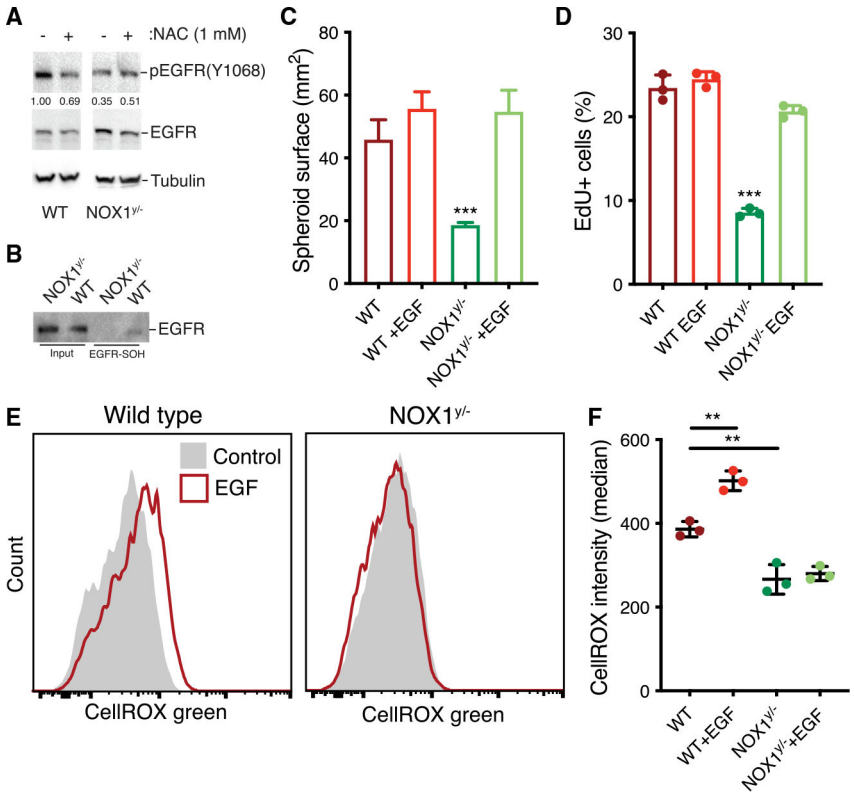

Figure 5. Basal NOX1-derived ROS regulate

(A) Western blot analysis of the EGFR phosphorylation status in WT and NOX1$^{y/-}$ spheroid cultures treated with 1 mM NAC. Values indicate the EGFR/phosphorylated EGFR (pEGFR) ratio changes compared with WT control.

(B) Sulfenylation status of EGFR in WT and NOX1$^{y/-}$ spheroid cultures was determined after incubation with DYn-2 for 1 h followed by biotin pull-down and western blot analysis. Data are represented as mean ± SEM.

(C) Surface of WT and NOX1$^{y/-}$ spheroids treated for 48 h with media supplemented with 50 ng/mL EGF (n = 3, 100 spheroids). Data are represented as mean ± SEM.

(D) EdU-positive cells determined by flow cytometry in WT and NOX1$^{y/-}$ spheroid cultures treated for 48 h with media containing 50 ng/mL EGF (n = 3).

(E) Representative flow cytometry plots of intracellular ROS detection in wild-type and NOX1$^{y/-}$ spheroids stimulated with EGF (50 ng/mL) for 1 h.

(F) Median CellROX fluorescent intensity of control and EGF-stimulated wild-type and NOX1 mutant spheroids as determined by flow cytometry (n = 3). Data are represented as mean ± SD.

**p < 0.001, ***p < 0.0001 by one-way ANOVA and Tukey's posttest.

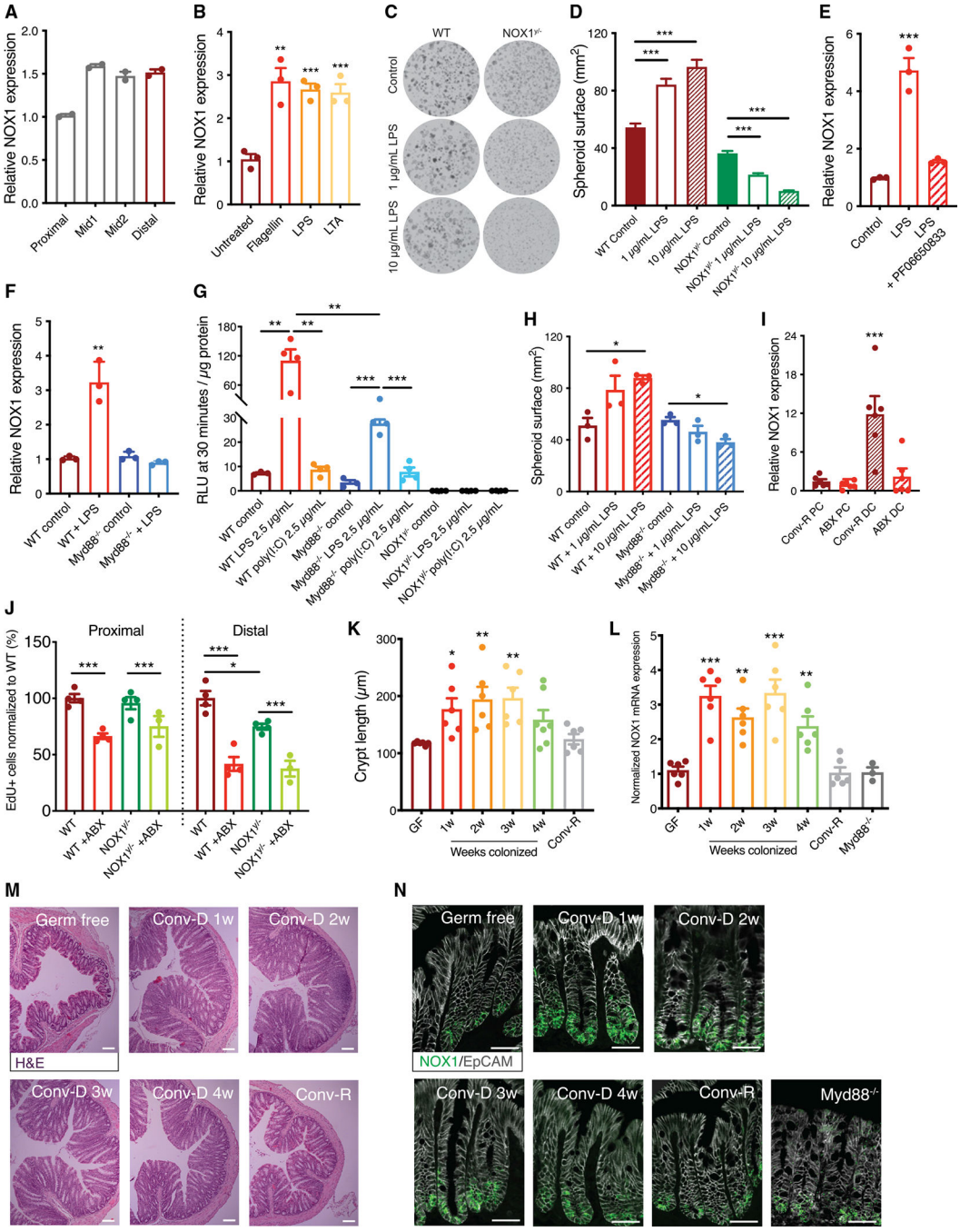

Figure 6. Microbial components induce TLR-dependent NOX1 expression and proliferation in colonic stem cells

(A) mRNA expression analysis for NOX1 expression in spheroid cultures after three passages established from four different segments between the proximal and distal colon (n = 2).

(B) Expression analysis for NOX1 in WT spheroids derived from the distal colon treated for 4 h with flagellin, LPS, or lipoteichoic acid (LTA) (n = 3).

(C) Representative whole-well stitched images of WT and NOX1$^{y/-}$ distal colon spheroids treated with 1 or 10 mg/mL LPS for 72 h (n = 3, 100 spheroids).

(D) Surface of WT and NOX1$^{y/-}$ distal colon spheroids treated with 1 or 10 mg/mL LPS for 72 h (n = 3, 100 spheroids).
(E) Expression analysis for NOX1 in WT spheroids pretreated for 30 min or untreated with the IRAK4 inhibitor (PF06650833) and stimulated for 4 h with LPS (n = 3).
(F) mRNA analysis for NOX1 mRNA expression in WT and Myd88$^{-/-}$ cultures in the presence of LPS for 4 h (n = 3).
(G) Superoxide generation as determined by L012 assay in WT, Myd88$^{-/-}$, and NOX1$^{y/-}$ colonic spheroids cultures overnight stimulated with the TLR ligands LPS or poly(I:C) (2.5 μg/mL) (n = 4).
(H) Spheroid surface of WT and Myd88$^{-/-}$ colonic-treated cultures with 1 or 10 μg/mL LPS for 72 h (n = 4).
(I) NOX1 expression in proximal and distal colon tissue in control and 1-week antibiotics-treated mice (n = 6).
(J) Quantification of the number of proliferative cells (EdU^{+}) in the PC and DC of WT and NOX1$^{y/-}$ mice after 1 week of broad-spectrum antibiotics treatment, as determined by flow cytometry analysis (n = 3–4).
(K) Crypt length as measurement for proliferation determined and measured in 12-week-old germ-free (GF) mice colonized with microbiota (Conv-D) from conventionally (Conv-R) raised mice (n = 6–7).
(L) Relative NOX1 mRNA expression analysis in distal colon tissue following a 4-week conventionalization period of germ-free mice compared with GF, Conv-R, and Myd88$^{-/-}$ mice (n = 6–7).
(M) Representative images of the different time points and conditions for the GF mice conventionalization experiment. Hematoxylin and eosin (H&E)-stained distal colon sections. Scale bars, 100 μM.
(N) *In situ* hybridization of NOX1 in colon tissue during 4-week conventionalization. GF, Conv-R, and Myd88$^{-/-}$ mice. Scale bars, 40 μm.
*p < 0.05, **p < 0.01, ***p < 0.001 by one-way ANOVA and Tukey's posttest. Data are represented as mean ± SEM.

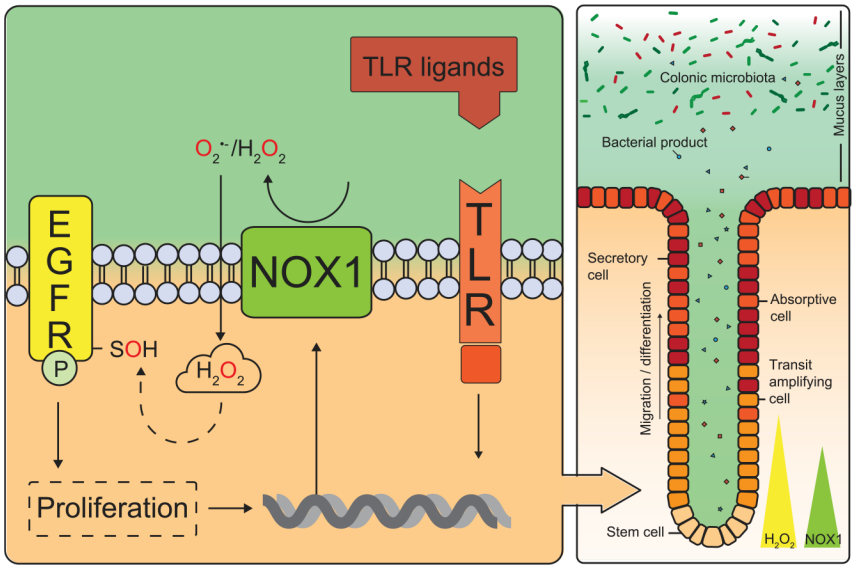

Figure 7. Proposed working model of NOX1 redox signaling in proliferative CSCs

The expression and ROS generation of NOX1 are restricted to the proliferating stem cells at the base of the colonic crypt. Basal NOX1-dependent ROS can redox-modify EGFR to potentiate its activation, which can be further enhanced via TLR stimulation that results in increased NOX1 expression. This feedback loop supports prolonged proliferation of colon stem cells by the presence of bacteria in the colonic lumen even in the absence of EGFR ligands.

KEY RESOURCES TABLE

REAGENT or RESOURCE	SOURCE	IDENTIFIER
Antibodies		
EGF Receptor	Cell Signaling	Cat# 2232, RRID: AB_331707
Phospho-EGF Receptor (Tyr1068)	Cell Signaling	Cat# 3777, RRID: AB_2096270
HRP goat anti-rabbit antibody	Sigma-Aldrich	Cat# 12–348, RRID: AB_390191
EpCAM	Abcam	Cat# ab71916, RRID: AB_1603782
A647 goat anti-rabbit antibody	Molecular probes	Cat# A-21245, RRID: AB_141775
Chemicals, peptides, and recombinant proteins		
5-Ethynyl-2'-deoxyuridine (EdU)	Cayman Chemicals	Cat# 20518
Y-27632	Cayman Chemicals	Cat# 10005583
L-161,982	Tocris	Cat# 2514
DAPT (γ-secretase inhibitor)	Sigma-Aldrich	Cat# 565770
Recombinant EGF (epidermal growth factor)	R&D systems	Cat# 236-EG
Ultrapure lipopolysaccharide (LPS)	InvivoGen	Cat# tlrl-3pelps
Flagellin	Sigma-Aldrich	Cat# SRP8029
Lipoteichoic acid (LPA)	Sigma-Aldrich	Cat# L3265
PF06650833	Sigma-Aldrich	Cat# PZ0327
Gefitinib	Cayman Chemicals	Cat# 13166
Sulfo-Cy5 azide	Lumiprobe	Cat# 3300
AF488-picolyl azide	Jena Bioscience	Cat# CLK-1276
CellROX green	ThermoFisher	Cat# C10444
Amplex ultrared reagent	ThermoFisher	Cat# A36006
ML171	Cayman Chemicals	Cat# 19056
L-012	FUJIFILM, Wako	Cat# 120–04891
Opal-570	Perkin-Elmer	Cat# FP1488001KT
DYn-2	Cayman Chemicals	Cat# 11220
Biotin picolyl azide	Click Chemistry Tools	Cat# 1167
THPTA (tris-hydroxypropyltriazolylmethylamine)	Click Chemistry Tools	Cat# 1010
Poly(I:C) HMW	Invivogen	Cat# tlr-pic
CF®488A Tyramide	Biotium	Cat# 92171
Critical commercial assays		
RNAscope fluorescent reagent kit v2	ACD, Bio-Techne	Cat# 323100
Experimental models: Cell lines		
Mouse: Colon organoids NOX1$^{y/-}$ (6 weeks, male)	This paper	N/A
Mouse: Colon organoids Myd88$^{-/-}$ (8 weeks, male)	This paper	N/A
Mouse: Colon organoids C57BL/6J (6 weeks, male)	This paper	N/A
Mouse: L-WRN	(Miyoshi and Stappenbeck, 2013)	CRL-3276, RRID: CVCL_DA06

REAGENT or RESOURCE	SOURCE	IDENTIFIER
Experimental models: Organisms/strains		
Mouse: NOX1$^{-/-}$	Jackson Laboratory	JAX:018787, RRID: IMSR_JAX:018787
Mouse: Myd88$^{-/-}$	(Adachi et al., 1998.)	N/A
Mouse: Lgr5-EGFP-IRES-creERT2	Jackson Laboratory	JAX:008875, RRID: IMSR_JAX:008875
Mouse: C57BL/6J	Jackson Laboratory	JAX:000664, RRID: IMSR_JAX:000664
Mouse: C57BL/6J (gnotobiotic)	Inhouse breeding	NA
Oligonucleotides		
NOX1 FISH-probe	ACD, Bio-Techne	Cat# 464651
Mki67 FISH-probe	ACD, Bio-Techne	Cat# 416771
qRT-PCR: 16S *universal* Forward: GGTGAATACGTTCCCGG	(Knoopetal., 2017)	N/A
qRT-PCR: 16S *universal* Reverse: TACGGCTACCTTGTTACGACTT	(Knoopetal., 2017)	N/A
qRT-PCR: *Actb* Forward: TGTGACGTTGACATCCGTAAAG	Integrated DNA technologies	Actb: *Mus musculus* NM_007393.5
qRT-PCR: Actb Reverse: TCAGTAACAGTCCGCCTAGAA	Integrated DNA technologies	Actb: *Mus musculus* NM_007393.5
qRT-PCR: Fabp1 Forward: TGTGGTCAGCTGTGGAAAG	Integrated DNA technologies	Fabp1: *Mus musculus* NM_017399
qRT-PCR: Fabp1 Reverse: GGCAGACCTATTGCCTTCAT	Integrated DNA technologies	Fabp1: *Mus musculus* NM_017399
qRT-PCR: *Ccnb1* Forward: CTGACCCAAACCTCTGTAGTG	Integrated DNA technologies	Ccnb1: *Mus musculus* NM_172301.3
qRT-PCR: Ccnb1 Reverse: CCTGTATTAGCCAGTCAATGAGG	Integrated DNA technologies	Ccnb1: *Mus musculus* NM_172301.3
qRT-PCR: *Duox2* Forward: ACGCAGCTCTGTGCTAAAGGT	Integrated DNA technologies	Duox2: *Mus musculus* NM_001362755.1
qRT-PCR: Duox2 Reverse: TGATGAACGAGACTCGACAGC	Integrated DNA technologies	Duox2: *Mus musculus* NM_001362755.1
qRT-PCR: *Gapdh* Forward: TGTCAAGCTCATTTCCTGGTAT	Integrated DNA technologies	Gapdh: *Mus musculus* NM_008084
qRT-PCR: Gapdh Reverse: GTGGTCCAGGGTTTCTTACTC	Integrated DNA technologies	Gapdh: *Mus musculus* NM_008084
qRT-PCR: *Lgr5* Forward: CGTAGGCAACCCTTCTCTTATC	Integrated DNA technologies	Lgr5: *Mus musculus* NM_010195.2
qRT-PCR: Lgr5 Reverse: GCACCATTCAAAGTCAGTGTTC	Integrated DNA technologies	Lgr5: *Mus musculus* NM_010195.2
qRT-PCR: *Mki67* Forward: ATTGACCGCTCCTTTAGGTATG	Integrated DNA technologies	Mki67: *Mus musculus* NM_001081117
qRT-PCR: Mki67 Reverse: TCGCCTTGATGGTTCCTTTC	Integrated DNA technologies	Mki67: *Mus musculus* NM_001081117
qRT-PCR: *Muc2* Forward: CCAGAAGGGACTGTGTATGATG	Integrated DNA technologies	Muc2: *Mus musculus* NM_023566.3
qRT-PCR: Muc2 Reverse: TGCTCACAGTCGTTGGTAAA	Integrated DNA technologies	Muc2: *Mus musculus* NM_023566.3
qRT-PCR: *Nos2* Forward: CTTGGTGAAAGTGGTGTTCTTTG	Integrated DNA technologies	Nos2: *Mus musculus* NM_010927.4
qRT-PCR: Nos2 Reverse: TCAGACTTCCCTGTCTCAGTAG	Integrated DNA technologies	Nos2: *Mus musculus* NM_010927.4
qRT-PCR: *Nox1* Forward: TCCAGTCTCCAAACATGACAG	Integrated DNA technologies	Nox1: *Mus musculus* NM_172203.2
qRT-PCR: *Nox1* Reverse: TTCCTGCGGATAAACTCCATAG	Integrated DNA technologies	Nox1: *Mus musculus* NM_172203.2
Software and algorithms		
Fiji/ImageJ	Open source program	https://imagej.net/FijiRRID: SCR_002285
Imaris	Bitplane	https://www.flowjo.com/RRID: SCR_008520
FlowJo v10	BD biosciences	https://www.flowjo.com/RRID: SCR_007370

REAGENT or RESOURCE	SOURCE	IDENTIFIER
Prism v8	GraphPad Software	https://www.graphpad.com/scientific-software/prism/RRID: SCR_002798